

A Lorentz Invariant Pairing Mechanism: Relativistic Cooper Pairs

A. Bermudez¹ and M.A. Martin-Delgado¹

¹*Departamento de Física Teórica I, Universidad Complutense, 28040. Madrid, Spain.*

We study a Lorentz invariant pairing mechanism that arises when two relativistic spin-1/2 fermions are subjected to a Dirac string coupling. In the weak coupling regime, we find remarkable analogies between this relativistic bound system and the well known superconducting Cooper pair. As the coupling strength is raised, quenched phonons become unfrozen and dynamically contribute to the gluing mechanism, which translates into novel features of this relativistic superconducting pair.

PACS numbers: 71.10.Li, 71.38-k, 03.65.Pm, 75.30.Ds

I. INTRODUCTION

A large class of superconducting materials can be accurately described by the BCS theory [1], which is based upon two major contributions. First, Frölich showed how the coupling between electrons and crystal phonons leads to an effective attractive interaction between the electrons [2]. Inspired by this result, Cooper discussed how any attractive interaction can bind a couple of electrons which lay around a filled Fermi sea [3]. This bound system, known as a Cooper pair, is responsible for several intriguing properties displayed by superconductors, which can be described as a many-body coherent state where electrons above the Fermi surface are bounded in pairs.

The oversimplified picture developed by Cooper captures the essence of the underlying physical phenomena occurring in superconducting solids. In the same spirit, we study a simple model of two relativistic fermions with an effective attractive interaction. In order to maintain the similarities with the Cooper problem, we must fulfill the two following requirements:

Phonon gluing mechanism: In a relativistic scenario, the simplest phonon-like coupling is modeled by a Dirac string coupling mechanism where the vibrations of the string describe the lattice phonons (see fig. 1 left). This interaction is introduced by a non-minimal coupling procedure in the free Dirac equation

$$i\hbar \frac{\partial |\Psi\rangle}{\partial t} = (c\boldsymbol{\alpha}(\mathbf{p} - im\omega\beta\mathbf{r}) + mc^2\beta) |\Psi\rangle, \quad (1)$$

where $|\Psi\rangle$ stands for the Dirac 4-component spinor, \mathbf{p} represents the momentum operator, and c the speed of light. Here $\beta = \text{diag}(\mathbb{I}_2, -\mathbb{I}_2)$, $\alpha_j = \text{off-diag}(\sigma_j, \sigma_j)$ are the Dirac matrices in the standard representation with σ_j as the usual Pauli matrices [4]. This Dirac string coupling $\mathbf{p} \rightarrow \mathbf{p} - im\omega\beta\mathbf{r}$ was introduced in [5, 6] as a relativistic extension of the harmonic oscillator, usually coined as the Dirac oscillator, where ω represents the oscillator's frequency. In our picture, this frequency effectively describes the lattice vibrations and its coupling to the fermionic degrees of freedom.

Two-fermion binding: Regardless of the coupling strength, we shall show that such an effective string coupling binds relativistic fermions in pairs (see fig. 1 right). A Lorentz invariant extension of the Dirac string

Hamiltonian in Eq.(1) to two-fermion systems is possible [7, 8, 9, 10], which in the center of mass reference frame reads as follows

$$H_{3D} = \frac{c}{\sqrt{2}}(\boldsymbol{\alpha}_1 - \boldsymbol{\alpha}_2)(\mathbf{p} - im\omega\beta_{12}\mathbf{r}) + mc^2(\beta_1 + \beta_2), \quad (2)$$

where $\boldsymbol{\alpha}_1 = \boldsymbol{\alpha} \otimes \mathbb{I}_4$, $\boldsymbol{\alpha}_2 = \mathbb{I}_4 \otimes \boldsymbol{\alpha}$, $\beta_1 = \beta \otimes \mathbb{I}_4$, $\beta_2 = \mathbb{I}_4 \otimes \beta$, and $\beta_{12} = \beta \otimes \beta$ represent the generalization of the Dirac matrices in the two-body Hilbert space. Here $\mathbf{p} := (\mathbf{p}_1 - \mathbf{p}_2)/\sqrt{2}$, and $\mathbf{r} := (\mathbf{r}_1 - \mathbf{r}_2)/\sqrt{2}$ stand for the relative momentum and position operators.

In this work, we study the binding properties of this two-body relativistic Hamiltonian, and discuss under which circumstances an analogy to Cooper pairs can be performed. Phonons in this relativistic system are dynamical and always provide a pairing mechanism, as we shall see. Thus, there is no need to invoke a many-body effect through the Pauli principle as in the original Cooper pair scenario. In fact, there are real materials which deviate from standard BCS theory. In BCS, phonons are quenched and their effect appears as a pairing energy scale, but they are not explicit in the Hamiltonian. There is an extension of the BCS theory that accounts for the effects of dynamical phonons, known as the Migdal-Eliashberg theory [11, 12, 13]. Our relativistic fermionic pairing mechanism is thus closer to this latter treatment.

We shall restrict ourselves to a two-dimensional system, where an exact solution is derived and several interesting properties can be neatly discussed. Two spa-

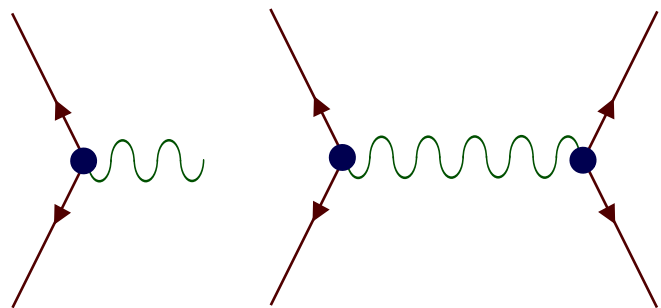


FIG. 1: (left) Electron-phonon interaction in the language of Feynman diagrams. (right) Effective electron-electron attractive interaction due to the exchange of a lattice phonon.

tial dimensions are also natural for other superconducting materials like the cuprates [14]. In this case, the Dirac matrices reduce to the usual Pauli matrices $\alpha_x = \sigma_x, \alpha_y = \sigma_y, \beta = \sigma_z$, and the relativistic 1-body state $|\Psi\rangle$ can be described by a 2-component spinor. The 2-body relativistic Hamiltonian in two dimensions can be written as follows

$$\begin{aligned} H_{2D} = & \frac{c}{\sqrt{2}}(\sigma_x \otimes \mathbb{I}_2 - \mathbb{I}_2 \otimes \sigma_x)(p_x - im\omega\sigma_z \otimes \sigma_z x) \\ & + \frac{c}{\sqrt{2}}(\sigma_y \otimes \mathbb{I}_2 - \mathbb{I}_2 \otimes \sigma_y)(p_y - im\omega\sigma_z \otimes \sigma_z y) \quad (3) \\ & + mc^2(\sigma_z \otimes \mathbb{I}_2 + \mathbb{I}_2 \otimes \sigma_z). \end{aligned}$$

II. ENERGY SPECTRUM AND EIGENSTATES

In two dimensions, chiral creation-annihilation operators which carry dual aspects of a left- or right-handed symmetry are defined as follows

$$\begin{aligned} a_r &:= \frac{1}{\sqrt{2}}(a_x - ia_y), & a_r^\dagger &:= \frac{1}{\sqrt{2}}(a_x^\dagger + ia_y^\dagger), \\ a_l &:= \frac{1}{\sqrt{2}}(a_x + ia_y), & a_l^\dagger &:= \frac{1}{\sqrt{2}}(a_x^\dagger - ia_y^\dagger), \end{aligned} \quad (4)$$

where $a_x^\dagger, a_x, a_y^\dagger, a_y$ are the usual creation-annihilation operators of the harmonic oscillator $a_i^\dagger = \frac{1}{\sqrt{2}}\left(\frac{1}{\Delta}r_i - i\frac{\tilde{\Delta}}{\hbar}p_i\right)$, and $\tilde{\Delta} = \sqrt{\hbar/m\omega}$ is related to the ground state width. Using these operators, the relativistic Hamiltonian in Eq. (3) takes a simpler and amenable form

$$H_{2D} = \begin{bmatrix} \Delta & g^* a_l^\dagger & g a_l^\dagger & 0 \\ g a_l & 0 & 0 & g^* a_r \\ g^* a_l & 0 & 0 & g a_r \\ 0 & g a_r^\dagger & g^* a_r^\dagger & -\Delta \end{bmatrix}, \quad (5)$$

where $\Delta := 2mc^2$ stands for the system rest mass, $g := imc^2\sqrt{2}\zeta$ is a coupling parameter, and $\zeta := \hbar\omega/mc^2$ controls the strength of the effective interaction. Considering the two-body spinorial basis $\{|\uparrow\uparrow\rangle, |\uparrow\downarrow\rangle, |\downarrow\uparrow\rangle, |\downarrow\downarrow\rangle\}$, we can understand the Dirac string coupling as a four-level system depicted in fig. 2.

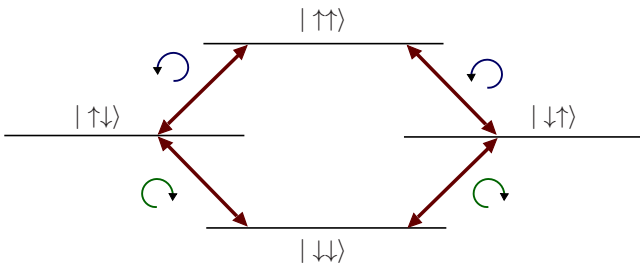


FIG. 2: Fermionic spin-flip transitions due to the Dirac string coupling and mediated by the creation-annihilation of chiral phonons.

We now proceed to describe the energy spectrum of the 2-body interacting relativistic system, in terms of the

phonon Fock states

$$|n_r, n_l\rangle := \frac{1}{\sqrt{n_r!n_l!}}(a_r^\dagger)^{n_r}(a_l^\dagger)^{n_l}|\text{vac}\rangle, \quad (6)$$

where $n_r, n_l = 0, 1, \dots$ specify the number of right- and left-handed phonons coupling the two-fermion system. One immediately observes that the Hilbert space can be divided in a series of invariant subspaces $\mathcal{H} = \bigoplus_{n_r, n_l=0}^{\infty} \mathcal{H}_{n_r, n_l}$, where each subspace can be described by $\mathcal{H}_{n_r, n_l} := \mathcal{H}'_{n_r, n_l} \oplus \mathcal{H}''_{n_r, n_l}$. These subspaces are spanned by

$$\begin{aligned} \mathcal{H}'_{n_r, n_l} &= \text{span}\{ |+\rangle |n_r, n_l\rangle \}, \\ \mathcal{H}''_{n_r, n_l} &= \text{span}\{ | \uparrow\uparrow \rangle |n_r, n_l + 1\rangle, |-\rangle |n_r, n_l\rangle, | \downarrow\downarrow \rangle |n_r + 1, n_l\rangle \}, \end{aligned} \quad (7)$$

where the states $|-\rangle := (|\uparrow\downarrow\rangle - |\downarrow\uparrow\rangle)/\sqrt{2}$, and $|+\rangle := (|\uparrow\downarrow\rangle + |\downarrow\uparrow\rangle)/\sqrt{2}$ are maximally entangled unpolarized Bell states. In particular, \mathcal{H}'_{n_r, n_l} describes a zero-energy subspace $E_{+, n_r, n_l} = 0$. The Hamiltonian (5) in the remaining subspaces \mathcal{H}''_{n_r, n_l} can be expressed as follows

$$H_{2D}^{n_r, n_l} = \Delta \begin{bmatrix} 1 & -i\sqrt{\zeta(n_l + 1)} & 0 \\ i\sqrt{\zeta(n_l + 1)} & 0 & -i\sqrt{\zeta(n_r + 1)} \\ 0 & i\sqrt{\zeta(n_r + 1)} & -1 \end{bmatrix}, \quad (8)$$

where the 2-body interaction couples three different levels and can be exactly diagonalized. Using Cardano-Vietta solution to third order polynomials, we obtain the following energies

$$\begin{aligned} \frac{E_{1n_r, n_l}}{\Delta} &:= \sqrt{\frac{4[1 + \zeta(n_r + n_l + 2)]}{3}} \cos \Theta, \\ \frac{E_{2n_r, n_l}}{\Delta} &:= \sqrt{\frac{4[1 + \zeta(n_r + n_l + 2)]}{3}} \cos \left(\Theta + \frac{2\pi}{3} \right), \\ \frac{E_{3n_r, n_l}}{\Delta} &:= \sqrt{\frac{4[1 + \zeta(n_r + n_l + 2)]}{3}} \cos \left(\Theta + \frac{4\pi}{3} \right), \end{aligned} \quad (9)$$

where

$$\Theta := \frac{1}{3} \arccos \left[\frac{27(n_l - n_r)\zeta}{2[3(1 + \zeta(n_r + n_l + 2))]^{3/2}} \right]. \quad (10)$$

These eigenstates are represented for different values of the coupling strength ζ in Fig. 3, where the chiral quantum numbers have been set to $n_r = n_l + 1$.

In this figure we observe two different regimes:

Weak Coupling regime $\zeta \ll 1$: In this case, the low energy properties can be accurately described by a two-level system. This feature will turn out to be crucial for the analogies of the system to a non-relativistic Cooper pair discussed in section III.

Strong Coupling regime $\zeta \gg 1$: In this case, the four levels become essential in order to describe the low energy excitations. Consequently, the description becomes more involved but also gives a richer structure that may show

certain novel properties with respect to non-relativistic Cooper pairs that are described in section IV.

Once the eigenvalues have been obtained, we may derive the corresponding eigenstates, which we list below

$$\begin{aligned} |E_{+,n_r,n_l}\rangle &:= |+,n_r,n_l\rangle, \\ |E_{j,n_r,n_l}\rangle &:= \frac{1}{\Omega_j} [\alpha_j |-\rangle |n_r,n_l\rangle + i\beta_j | \uparrow\uparrow, n_r, n_l + 1\rangle \\ &\quad + i\delta_j | \downarrow\downarrow, n_r + 1, n_l\rangle], \end{aligned} \quad (11)$$

where we have defined the following parameters

$$\begin{aligned} \alpha_j &:= \Delta^2 - E_{jn_r,n_l}^2, \\ \beta_j &:= \Delta(\Delta + E_{jn_r,n_l})\sqrt{\zeta(n_l + 1)}, \\ \delta_j &:= \Delta(\Delta - E_{jn_r,n_l})\sqrt{\zeta(n_r + 1)}, \\ \Omega_j &:= \sqrt{\alpha_j^2 + \beta_j^2 + \delta_j^2}. \end{aligned} \quad (12)$$

Here the indexes $j = 1, 2, 3$ correspond to the three different eigenvalues (9). Let us mention that the total angular momentum $J_z := S_z + L_z$ is conserved. Thus, the eigenstates (11) have well-defined angular momenta, namely, $\hbar(n_r - n_l)$. Finally, we must consider the consequences of fermion indistinguishability. The Symmetrization postulate states that a system of identical fermions must be described in terms of antisymmetrical states, which establishes the following constraint

$$P_{21}|\Psi(1, 2)\rangle = -|\Psi(1, 2)\rangle, \quad (13)$$

where P_{21} stands for the permutation operator that swaps the fermion labels $1 \leftrightarrow 2$. Considering the eigenstates in Eq.(11) under the permutation operator, we obtain the following expressions

$$\begin{aligned} P_{21}|E_{+,n_r,n_l}\rangle &= (-1)^{n_r+n_l}|E_{+,n_r,n_l}\rangle, \\ P_{21}|E_{j,n_r,n_l}\rangle &= (-1)^{n_r+n_l+1}|E_{j,n_r,n_l}\rangle. \end{aligned} \quad (14)$$

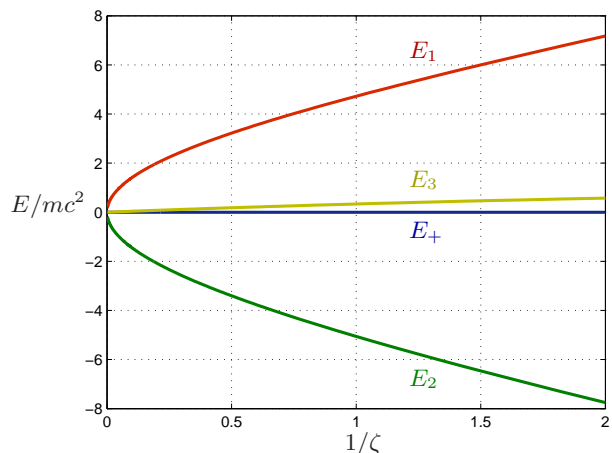


FIG. 3: Dependence of the two-fermion energy spectrum with the Dirac string coupling strength. Note that as $1/\zeta \rightarrow 0$ we approach the strong coupling regime $\zeta \gg 1$, whereas $1/\zeta \rightarrow \infty$ represents a weak attractive coupling $\zeta \ll 1$.

Since these expressions must satisfy the antisymmetric condition in Eq.(13), the number of chiral quanta are constrained as follows

$$\begin{aligned} |E_{+,n_r,n_l}\rangle &\Rightarrow n_r + n_l = 2k + 1 \quad : k = 0, 1, 2, \dots \\ |E_{j,n_r,n_l}\rangle &\Rightarrow n_r + n_l = 2k \quad : k = 0, 1, 2, \dots \end{aligned} \quad (15)$$

Due to the indistinguishability of the relativistic fermions, the eigenstates $|E_{+,n_r,n_l}\rangle$ must contain an odd number of chiral quanta, whereas $|E_{j,n_r,n_l}\rangle$ are restricted to even number of chiral quanta.

We have thus derived a complete solution of the relativistic Dirac equation for two bodies interacting via a Dirac string coupling. Therefore, this 2-fermion system belongs to the small class of exactly solvable few-body relativistic systems. In sections III and IV we show that this relativistic interaction does indeed lead to the formation of bound pairs, both in the weak and strong coupling regimes. Furthermore, we present a detailed study of the similar properties that the relativistic bound pair shares with the well-known non-relativistic Cooper pair. As we will see, there are profound analogies in the weak coupling regime, whereas novel properties are found in the strong coupling limit.

III. WEAK COUPLING REGIME

The standard description of Cooper pairs in superconducting solids is usually performed in a weak coupling regime, where a slightly phonon-mediated attractive interaction binds electron which lay close to the Fermi surface. We shall consider that the two-body Hamiltonian in Eq. (3) effectively describes the gluing mechanism above the Fermi sea, and therefore a weak coupling regime is obtained when $\zeta \ll 1$.

In this weak coupling regime, we have seen in Fig. 3 that the low-lying excitations can be entirely described by a two-level system. This situation is schematically described fig. 4, where we see how spin-polarized levels become decoupled from those responsible of the low-energy properties. In this situation, we can obtain an effective Hamiltonian for the low energy sector, by adiabatic elimination.

Let us consider an arbitrary state $|\Psi(t)\rangle \in \mathcal{H}_{n_r,n_l}$

$$\begin{aligned} |\psi(t)\rangle &= c_{\uparrow\uparrow}(t) | \uparrow\uparrow, n_r, n_l + 1\rangle + c_{\uparrow\downarrow}(t) | \uparrow\downarrow, n_r, n_l\rangle \\ &\quad + c_{\downarrow\uparrow}(t) | \downarrow\uparrow, n_r, n_l\rangle + c_{\downarrow\downarrow}(t) | \downarrow\downarrow, n_r + 1, n_l\rangle, \end{aligned} \quad (16)$$

whose dynamical evolution, described by the Dirac Hamiltonian (5), can be represented as

$$i\hbar \frac{d}{dt} \begin{bmatrix} c_{\uparrow\uparrow}(t) \\ c_{\uparrow\downarrow}(t) \\ c_{\downarrow\uparrow}(t) \\ c_{\downarrow\downarrow}(t) \end{bmatrix} = \begin{bmatrix} \Delta & g^* a_l^\dagger & g a_l^\dagger & 0 \\ g a_l & 0 & 0 & g^* a_r \\ g^* a_l & 0 & 0 & g a_r \\ 0 & g a_r^\dagger & g^* a_r^\dagger & -\Delta \end{bmatrix} \begin{bmatrix} c_{\uparrow\uparrow}(t) \\ c_{\uparrow\downarrow}(t) \\ c_{\downarrow\uparrow}(t) \\ c_{\downarrow\downarrow}(t) \end{bmatrix}. \quad (17)$$

In the weak coupling limit, the transitions to the spin-polarized $\{|\uparrow\uparrow, n_r, n_l + 1\rangle, |\downarrow\downarrow, n_r + 1, n_l\rangle\}$ upper and lower levels can be considered negligible. Therefore, the level population does not evolve under the action of the two-body interaction $\frac{dc_{\uparrow\uparrow}}{dt} = \frac{dc_{\downarrow\downarrow}}{dt} = 0$, and we can adiabatically eliminate these two levels. The latter conditions substituted in Eq. (17), give rise to the following relations

$$\begin{aligned} c_{\uparrow\uparrow} &= i\sqrt{\frac{\zeta(n_l + 1)}{2}}(c_{\uparrow\downarrow} - c_{\downarrow\uparrow}), \\ c_{\downarrow\downarrow} &= i\sqrt{\frac{\zeta(n_r + 1)}{2}}(c_{\uparrow\downarrow} - c_{\downarrow\uparrow}), \end{aligned} \quad (18)$$

and an effective two-level dynamics

$$i\hbar \frac{d}{dt} \begin{bmatrix} c_{\uparrow\downarrow}(t) \\ c_{\downarrow\uparrow}(t) \end{bmatrix} = \frac{\Delta\zeta}{2}(n_r - n_l) \begin{bmatrix} 1 & -1 \\ -1 & 1 \end{bmatrix} \begin{bmatrix} c_{\uparrow\downarrow}(t) \\ c_{\downarrow\uparrow}(t) \end{bmatrix}. \quad (19)$$

In this sense, we can integrate out the high-frequency modes by projecting onto the effective spin-unpolarized invariant subspace spanned by $\mathcal{H}_{n_r, n_l}^{\text{eff}} := \text{span}\{|\uparrow\downarrow, n_r, n_l\rangle, |\downarrow\uparrow, n_r, n_l\rangle\}$, by means of an orthogonal projector

$$\mathcal{P}_{n_r, n_l}^{\text{eff}} := |\uparrow\downarrow, n_r, n_l\rangle\langle\uparrow\downarrow, n_r, n_l| + |\downarrow\uparrow, n_r, n_l\rangle\langle\downarrow\uparrow, n_r, n_l| \quad (20)$$

The z -component of the orbital angular momentum operator $L_z = \hbar(a_r^\dagger a_r - a_l^\dagger a_l)$ constrained to this invariant subspace becomes $\mathcal{P}_{n_r, n_l}^{\text{eff}} L_z \mathcal{P}_{n_r, n_l}^{\text{eff}} = \hbar(n_r - n_l)\mathbb{I}_2$, which allows us to rewrite Eq. (19) as an effective two-level Hamiltonian

$$H_{\text{eff}} := \omega L_z \begin{bmatrix} 1 & -1 \\ -1 & 1 \end{bmatrix} = \hbar\omega(a_r^\dagger a_r - a_l^\dagger a_l) \begin{bmatrix} 1 & -1 \\ -1 & 1 \end{bmatrix}. \quad (21)$$

This effective interaction in the weak coupling regime is represented in Fig. 4, where the allowed transitions

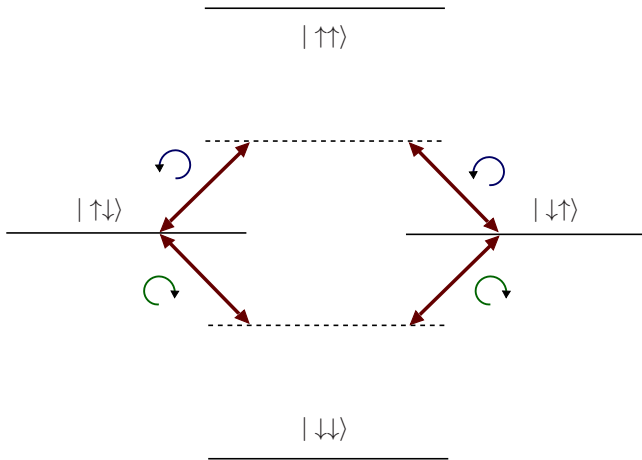


FIG. 4: Fermionic spin-flip transitions in the weak coupling regime. The low energy sector is described by an effective two-level system, where spin-flips occur along two different channels that include virtual two-phonon transitions and spin-polarized states become decoupled.

can take on two different channels via the consecutive creation-annihilation of right- or left-handed phonons. This process can be understood as an instance of a superexchange coupling between the spins $|\uparrow\downarrow\rangle \leftrightarrow |\downarrow\uparrow\rangle$ driven by a second order two-phonon process where a chiral phonon is virtually created and then annihilated. There exist two different exchange paths, as seen in fig. 4, depending on the left- or right-handed chiralities of the virtual phonons involved in the process.

This effective Hamiltonian (21) can be exactly diagonalized yielding the eigenvalues

$$E_{+n_r, n_l}^{\text{eff}} := 0, \quad E_{-n_r, n_l}^{\text{eff}} := 2\hbar\omega(n_r - n_l), \quad (22)$$

with the following associated eigenstates

$$\begin{aligned} |E_{+n_r, n_l}^{\text{eff}}\rangle &:= |+, n_r, n_l\rangle \Rightarrow n_r + n_l = 2k + 1 \quad : k = 0, 1, 2, \dots \\ |E_{-n_r, n_l}^{\text{eff}}\rangle &:= |-, n_r, n_l\rangle \Rightarrow n_r + n_l = 2k \quad : k = 0, 1, 2, \dots \end{aligned} \quad (23)$$

where the anti-symmetric character of the fermionic states has already been considered. Therefore, the low-lying solution in the weak coupling regime can be described by the maximally entangled Bell states in the spin degree of freedom, and rotational Fock states in the orbital degree of freedom.

Furthermore, these states describe a bound fermion pair. In order to show that such binding occurs, we must show that the inter-particle distance only attains finite values. Let us introduce the square-distance operator $\Gamma := x^2 + y^2$, where $x := (x_1 - x_2)/\sqrt{2}$ and $y := (y_1 - y_2)/\sqrt{2}$ denote the space coordinate operators for the relative fermionic distance. The expectation values in the weak-coupling eigenstates (23) are

$$\langle\Gamma\rangle_{\pm} = \frac{\tilde{\Delta}^2}{\sqrt{2}}(1 + n_r + n_l), \quad (24)$$

which is always finite. We observe the crucial property that this system shares with a non-relativistic Cooper pair, namely, the pair of relativistic fermions are bounded in pairs even for a weak attraction $\zeta \ll 1$.

Another fundamental property that occurs in standard Cooper pairs is the presence of an energy gap between the paired energy level and the Fermi surface. This energy gap is responsible of the stability of Cooper pairs with respect to free fermion pairs and is proportional to the lattice Debye frequency $\Delta E \sim \hbar\omega_D$. In the relativistic regime, we observe that the energy gap with respect to the displaced Fermi surface (i.e. $\epsilon'_F = 0$) is

$$\begin{aligned} \Delta E_{+n_r, n_l} &= 0, \\ \Delta E_{-n_r, n_l} &= 2\hbar\omega(n_r - n_l), \end{aligned} \quad (25)$$

and therefore the only stable pair (i.e. $\Delta E < 0$) is that described by the spin-singlet state when $n_l \geq n_r$.

In this sense we obtain a spin-singlet bound pair which clearly resembles the situation in standard Cooper pairs

where the fermions are also in the singlet state. Furthermore, we can observe from this discussion that the relativistic gap is proportional to the Dirac string frequency $\Delta E \sim \hbar\omega$, which plays the role of the usual Debye frequency in superconducting materials.

Finally, to take this comparison further, we should study the properties of the stable pair eigenstates in Eq. (23) and compare them to the non-relativistic Cooper pair features.

Spin degrees of freedom: In BCS theory, Cooper pairs display a singlet state in the spin degree of freedom. We observe in Eq. (23) that the stable bound fermionic pair state has also a spin-singlet component.

Orbital degrees of freedom: In BCS theory, Cooper pairs display a spherically symmetrical wave function with an onion-like layered structure. We directly observe from fig. 5 that relativistic bound pair probability distribution $\rho_{-n_r, n_l}^{\text{eff}}(r)$ display a similar spherically symmetric onion-like structure.

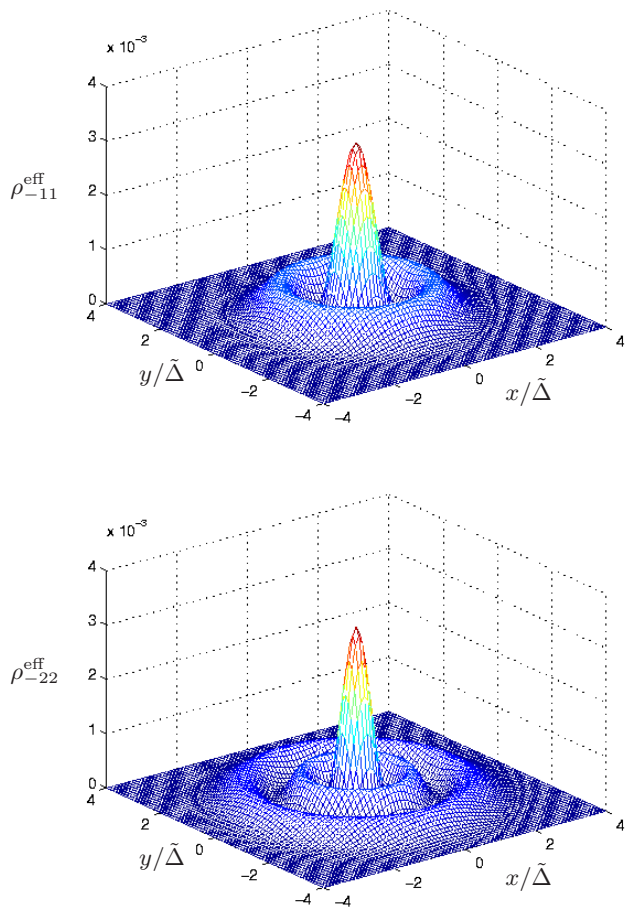


FIG. 5: Spatial probability density profiles for weak coupling stable pairs $\rho_{-n_r, n_l}^{\text{eff}}(r) := \text{Tr}_{\text{spin}}(\langle \mathbf{r} | E_{-n_r, n_l}^{\text{eff}} \rangle \langle E_{-n_r, n_l}^{\text{eff}} | \mathbf{r} \rangle)$ with $n_l > n_r$. Top figure corresponds to $n_r = 1, n_l = 1$ probability density $\rho_{-11}^{\text{eff}}(r)$, with $r = |\mathbf{r}_1 - \mathbf{r}_2|/\sqrt{2}$. Bottom figure represents $\rho_{-22}^{\text{eff}}(r)$.

In this section we have discussed a relativistic pairing mechanism in a weak coupling regime. We have discussed in detail several analogies with a non-relativistic Cooper pair that naturally arise in this weak coupling limit. Remarkably, we obtain binding regardless of the interaction strength, which is a fundamental property of BCS systems. Additionally, we have shown how the relativistic energy gap scales with the string frequency in the same manner as the Cooper pair gap scales with the phonon Debye frequency. In this regard, we may conclude that the string interaction plays the role of the lattice phonons that mediate the effective attraction between fermions in the BCS theory. Furthermore, we have also compared the nature of the relativistic pair eigenstates with the Cooper pair wave functions. We have seen that the relativistic bound pair is also described by a spin-singlet state and a spherically symmetric onion-like state in the orbital degrees of freedom. All these similarities allow us to state that this fermionic pairing mechanism can be interpreted as a relativistic Cooper pair, since we recover most of the usual BCS properties in the weak coupling regime. Nonetheless, this Relativistic Cooper pair can also be studied in the strong coupling regime, where novel properties with respect to the usual Cooper pair in BCS theory arise. As we describe below, when the Dirac string interaction becomes strong enough, phonons contribute dynamically to the gluing mechanism.

IV. STRONG COUPLING REGIME

In this section we study the pairing properties of the two-body relativistic system in the strong coupling regime $\zeta \gg 1$. In this limit we must consider the complete four-level structure of the system (see fig. 2), and the energy spectrum becomes clearly more involved in Eq. (9) (see fig. 6).

In fig. 6 we have represented the different energies for an interaction strength $\zeta = 5$ which lays in the strong coupling regime. We clearly see how two levels $E_{2, n_r, n_l}, E_{3, n_r, n_l}$ become stable pairs with a certain gap $\Delta E_{2, n_r, n_l} < \Delta E_{3, n_r, n_l} < 0$. Therefore the strong coupling gives raise to a couple of stable bound fermionic states, namely,

$$\begin{aligned}
 |E_{2, n_r, n_l}\rangle &:= \frac{1}{\Omega_2} [\alpha_2 |-\rangle |n_r, n_l\rangle + i\beta_2 | \uparrow\uparrow, n_r, n_l + 1\rangle + \\
 &\quad + i\delta_2 | \downarrow\downarrow, n_r + 1, n_l\rangle]; \\
 |E_{3, n_r, n_l}\rangle &:= \frac{1}{\Omega_3} [\alpha_3 |-\rangle |n_r, n_l\rangle + i\beta_3 | \uparrow\uparrow, n_r, n_l + 1\rangle + \\
 &\quad + i\delta_3 | \downarrow\downarrow, n_r + 1, n_l\rangle].
 \end{aligned}
 \tag{26}$$

The spatial probability distribution $\rho_{j n_r n_l}(r)$ of these stable fermionic pairs has been represented in fig. 7 in the case of $n_r = n_l = 1$. We can clearly observe that the density profile preserves the spherically symmetric onion-like structure. Nonetheless, noteworthy differences arise

with respect to the weak coupling regime (compare to the top fig. 5).

Furthermore, these two stable states form a fermionic bound pair since the inter-particle distance is finite

$$\begin{aligned} \langle \Gamma \rangle_2 &= \tilde{\Delta}^2 [(1 + n_r + n_l)\alpha_2^2 + (\beta_2^2 + \delta_2^2)(2 + n_r + n_l)], \\ \langle \Gamma \rangle_3 &= \tilde{\Delta}^2 [(1 + n_r + n_l)\alpha_3^2 + (\beta_3^2 + \delta_3^2)(2 + n_r + n_l)]. \end{aligned} \quad (27)$$

We may conclude that the Dirac string pairing mechanism leads to bound pairs in the strong coupling regime, which display substantial differences with respect to the weakly coupled bound states in Eq. (23). It follows from Eqs. (26) that the bound pairs are not in a singlet state but rather in a linear superposition of different spin singlet and triplet states entangled with different orbital Fock states. In this regard, the relativistic pairing mechanism does not induce an anti-ferromagnetic ordering any longer, and certain spin-polarization may arise depending on the value of the coupling strength ζ .

It is also instructive to compare the orbital degrees of freedom of bound pairs in the weak and strong coupling limits. The weakly coupled states in Eq. (23) are in orbital Fock states, which represent a certain number of vibrational phonons which are frozen in this limit. On the other hand, strongly coupled states in Eqs. (26) cannot be described by a single Fock state, and therefore the vibrational phonons acquire a dynamical behavior $|n_r + 1, n_l\rangle \Leftrightarrow |n_r, n_l\rangle \Leftrightarrow |n_r, n_l + 1\rangle$, which is a clear sign of strong coupling in superconductors. We may conclude that the Dirac string phonons, responsible of the gluing mechanism, become unfrozen as the coupling be-

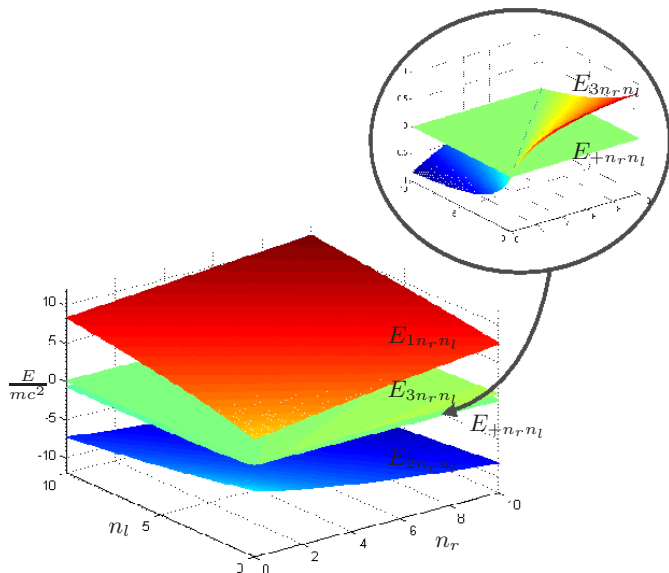


FIG. 6: Energy levels of the two-body Dirac oscillator in the strong coupling regime $\zeta = 5$ as a function of the different phonon number.(inset) Detail of the energies corresponding to levels $E_{+n_r n_l}$, $E_{3n_r n_l}$

comes stronger and contribute to the effective attraction in a dynamic phenomenon. This is reminiscent of a (s, p) -wave symmetry of a SC order parameter. Similar types of superconducting states appear in some quantum liquids like superfluid He^3 : the so-called A- and B-phases exhibit different patterns of spin-orbit symmetry breaking [15, 16]. Layered materials like the ruthenates also exhibit unusual symmetry properties like triplet superconductivity [17, 18, 19].

We also observe that the strong pairing mechanism leads to a couple of possible stable bound pairs (26), whereas the weak coupling only produces one stable bound pair. Furthermore, the energy gap displayed by the bound pairs also depends on the strength of the coupling. In the weak coupling regime, we have already seen that the energy gap scales as $\Delta E_- \sim \hbar\omega$, whereas the scaling in the strongly interaction limit does not present such a simple scaling (see fig. 6).

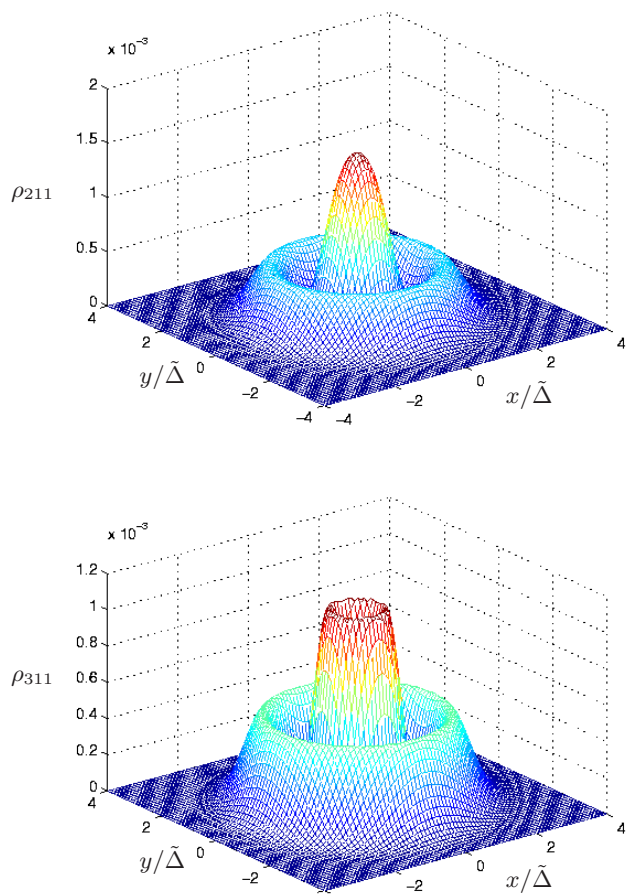


FIG. 7: Spatial probability density profiles for strong coupling $\zeta = 5$ stable pairs $\rho_{jn_r n_l}(r) := \text{Tr}_{\text{spin}}(\langle \mathbf{r} | E_{jn_r n_l} \rangle \langle E_{jn_r n_l} | \mathbf{r} \rangle)$ with $n_r = 1, n_l = 1$. Top figure corresponds to the probability density of the stable pair $\rho_{211}(r)$, with $r = |\mathbf{r}_1 - \mathbf{r}_2|/\sqrt{2}$. Bottom figure represents the probability density of the stable pair $\rho_{311}(r)$.

V. CONCLUSIONS

We have studied the relativistic pairing mechanism of the two-body Dirac oscillator in two dimensions, where a Dirac string coupling leads to fermionic bound pairs. We have described two different regimes where binding occurs regardless of the interaction strength.

In a weak coupling regime, the fermionic pair bears a strong resemblance to the usual Cooper pair in BCS theory. We remarkably found a similar scaling of the energy gap, which allows us to identify the Dirac string frequency ω with the lattice phonon Debye frequency ω_D in superconducting materials. Additionally, we found that the relativistic bound pair eigenstates are also in a spin singlet state, and present a spherically symmetric onion-like structure in the probability distribution. All these remarkable analogies suggest to interpret this two-body

Dirac oscillator as an instance of a relativistic Cooper pair. Nevertheless, there may also be other types of relativistic binding mechanisms yielding also the formation of Cooper pairs.

On the other hand, a strong interaction leads to remarkable differences with respect to BCS Cooper pairs. In this case, more than one bound pair can be built, which in any case is not in a singlet state but rather in a linear superposition of singlet and triplet states. Furthermore, the gluing phonons become unfrozen as the coupling strength is raised and dynamically contribute to the pairing mechanism.

Acknowledgements We acknowledge financial support from a FPU grant of the MEC (A.B.), DGS grant under contract FIS2006-04885, CAM-UCM grant under ref. 910758. (A.B., M.A.M.D.), and the ESF Science Programme INSTANS 2005-2010 (M.A.M.D.).

-
- [1] J. Bardeen, L. N. Cooper, and J. R. Schrieffer, Phys. Rev. **108**, 1175 (1957).
 [2] H. Fröhlich, Phys. Rev. **79**, 845 (1950).
 [3] L. N. Cooper, Phys. Rev. **104**, 1189 (1956).
 [4] W. Greiner, “*Relativistic Quantum Mechanics. Wave Equations.*”, (Springer, Berlin, 2000).
 [5] D. Ito, K. Mori, and E. Carrieri, N. Cimento **51 A**, 1119, (1967).
 [6] M. Moshinsky, and A. Szczepaniak, J. Phys. A **22**, L817, (1989).
 [7] A. O. Barut, and S. Komy, Fortsch. Phys. **33**, 6 (1985).
 [8] M. Moshinsky, G. Loyola, and C. Villegas, J. Math. Phys. **32**, 373 (1990).
 [9] M. Moshinsky, and G. Loyola, Found. Phys. **23**, 197 (1993).
 [10] A. González, G. Loyola, and M. Moshinsky, Rev. Mex. Fis. **40**, 12 (1994).
 [11] A.B. Migdal, Zh. Eksp. Teor. Fiz., **34**, 1438 (1958); (Sov. Phys. JETP, **7**, 996 (1958)).
 [12] G.M. Eliashberg, Zh. Eksp. Teor. Fiz., **38**, 966 (1960); **39**, 1437 (1960); (Sov. Phys. JETP, **11**, 696 (1960); **12**, 1000 (1960)).
 [13] J.P. Carbotte, Rev. Mod. Phys. **62**, 1027 (1990).
 [14] J.G. Bednorz, and K. A. Müller, Z. Phys. B **64**, 189 (1986).
 [15] D.D. Osheroff, R.C. Richardson, and D.M. Lee, Phys. Rev. Lett. **28**, 885 (1972).
 [16] A.J. Leggett, Rev. Mod. Phys. **47**, 331 (1975).
 [17] Y. Maeno et al., Nature **372**, 532 (1994).
 [18] T. M. Rice, and M. Sigrist, J. Phys. Cond. Matter **7**, L643 (1995).
 [19] G. Baskaran, Physica B 223-224, 490 (1996).